RRO COMPENSATION OF HARD DISK DRIVES WITH MULTIRATE REPETITIVE PTC

Hiroshi Fujimoto *

* *Department of Electrical and Computer Engineering, Yokohama National University, Yokohama 240-8501, Japan hfuji@ieee.org*

Abstract: In this paper, novel repetitive controllers are proposed based on perfect tracking control (PTC) in order to reject high-order repeatable runout (RRO) of hard disk drives. First, the feedback approach of the repetitive PTC (RPTC) is developed with internal model of periodic disturbance. Although this method has performance robustness against small plant variation, the internal model worsens the stability robustness for big modeling error. Then, the feedforward approach of RPTC is introduced with switching mechanism such that the high-order RRO can be rejected without any sacrifice of the closed-loop characteristics. In both approaches, multirate feedforward control is utilized to overcome the unstable zero problem of discrete-time plant. Finally, the advantages and disadvantages are demonstrated through simulations and experiments.

Keywords: multirate control, repetitive control, hard disk drive, switching mechanism

1. INTRODUCTION

In the head-positioning system of hard disk drives (HDDs), the head position is detected by the discrete servo signals embedded in the disks. Thus, the control period (T_u) to update the force command signal can be set shorter than the sampling period (T_y) of position error signal. Therefore, multirate controllers with the constraint of $T_u < T_y$ have been applied both to track-seeking and track-following modes in HDDs [Takakura, 1999, Wu and Tomizuka, 2003, Lee and Tomizuka, 2003, Hirata et al., 2003]. The author has applied perfect tracking control (PTC) to seeking mode with multirate feedforward compensation [Fujimoto et al., 1999]. This paper applies PTC to track-following mode. In this mode, two-degree-of-freedom (2DOF) controller is generally supposed to be inapplicable since the reference signal called track runout is immeasurable in HDDs. However, this paper introduces novel control schemes with switching mechanism and feedforward compensation, which makes the 2DOF PTC be applicable to repeatable runout rejection control of track-following mode.

Repetitive control is a widely used technique to reject periodic disturbances or to track a periodic reference signal [Chew and Tomizuka, 1990, Hara et al., 1988]. Although this control scheme has excellent performance for low order disturbance modes, it cannot reject relatively higher frequency modes. The reasons of this difficulty are (1) the delay caused by zero-order hold of plant input when the high-order mode is close to Nyquist frequency, (2) the low-pass filter is required to maintain the stability robustness, and (3) approximated inverse is implemented to deal with the unstable zero of discrete-time plant in the conventional discrete-time repetitive controller [Chew and Tomizuka, 1990]. This paper overcomes these problems by introducing novel control schemes named repetitive perfect tracking control (RPTC).

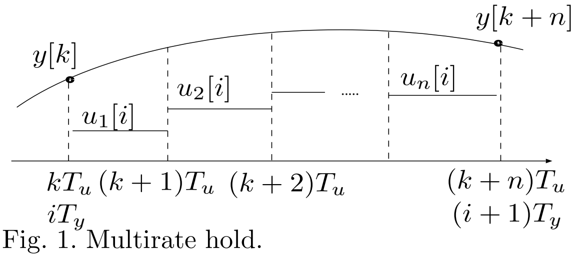

Fig. 1. Multirate hold.

The recent development of computer technology enabled to set the control period T_u shorter than the sampling period T_y when the sensor speed is restricted. In this paper, the above-mentioned problem (1) is overcome by the multirate input control ($T_u < T_y$).

In the conventional digital repetitive control [Chew and Tomizuka, 1990], the discrete-time disturbance model $(z^{N_d} - 1)^{-1}$ is implemented in feedback-loop as the internal model. Although the sensitivity function becomes zero at the disturbance harmonics frequencies, the sensitivity has big amplitude at the other frequency band, which causes severe damage in total tracking accuracy. Moreover, the closed-loop system could become unstable because the peak gain of internal model excites the unmodeled dynamics. Therefore, low-pass filter is usually implemented in repetitive control to assure the stability robustness at the sacrifice of high-frequency disturbance rejection performance. On the other hand, this paper introduces novel switching schemes to achieve repetitive disturbance rejection by feedforward control.

The problem (3) of discrete-time unstable zero was not crucial in the conventional feedback repetitive control because the stability can be assured even when the approximated zero-phase-error (ZPE) inverse is utilized [Chew and Tomizuka, 1990]. However, when the feedforward scheme is introduced with switching scheme, the gain characteristics of ZPE [Tomizuka, 1987] causes the tracking error especially for high-order disturbance. Therefore, in the proposed methods, the perfect tracking control which was proposed by authors in Fujimoto et al. [2001] is utilized with multirate input control to obtain the ideal inner-loop system in discrete-time domain.

2. REPETITIVE PERFECT TRACKING CONTROL (RPTC)

In this paper, it is assumed that the control input can be changed N times during the sampling period of output signal T_y. For simplification, the input multiplicity N is set to be equal with the order of nominal plant n since $N \geq n$ is the necessary condition of perfect tracking [Fujimoto et al., 2001]. But, by using the formulation of Fujimoto et al. [2001], this assumption can be relaxed to deal with more general system with $N \neq n$.

Consider the continuous-time nth-order plant described by

$$\dot{\boldsymbol{x}}(t) = \boldsymbol{A}_c\boldsymbol{x}(t) + \boldsymbol{b}_c u(t), \quad p(t) = \boldsymbol{c}_c\boldsymbol{x}(t) \tag{1}$$

The discrete-time state equation discretized by the shorter period T_u becomes

$$\boldsymbol{x}[k+1] = \boldsymbol{A}_s\boldsymbol{x}[k] + \boldsymbol{b}_s u[k], \tag{2}$$

where $\boldsymbol{x}[k] = \boldsymbol{x}(kT_u)$ and

$$\boldsymbol{A}_s := e^{\boldsymbol{A}_c T_u}, \quad \boldsymbol{b}_s := \int_0^{T_u} e^{\boldsymbol{A}_c\tau}\boldsymbol{b}_c d\tau. \tag{3}$$

By calculating the state transition from $t = iT_y = kT_u$ to $t = (i+1)T_y = (k+n)T_u$ in Fig. 1, the discrete-time plant $P[z]$ can be represented by

$$\boldsymbol{x}[i+1] = \boldsymbol{A}\boldsymbol{x}[i] + \boldsymbol{B}\boldsymbol{u}[i], \quad p[i] = \boldsymbol{c}\boldsymbol{x}[i], \tag{4}$$

where $\boldsymbol{x}[i] = \boldsymbol{x}(iT_y), z := e^{sT_y}$, and multirate input vector $\boldsymbol{u}$ is defined in the lifting form as

$$\begin{aligned}\boldsymbol{u}[i] &:= [u_1[i], \cdots, u_n[i]]^T \\ &= [u(kT_u), \cdots, u((k+n-1)T_u)]^T\end{aligned} \tag{5}$$

and the coefficients are given by

$$\boldsymbol{A} = \boldsymbol{A}_s^n, \boldsymbol{B} = [\boldsymbol{A}_s^{n-1}\boldsymbol{b}_s, \boldsymbol{A}_s^{n-2}\boldsymbol{b}_s, \cdots, \boldsymbol{A}_s\boldsymbol{b}_s, \boldsymbol{b}_s], \tag{6}$$
$$\boldsymbol{c} = \boldsymbol{c}_c.$$

2.1 Design of RPTC

In Fujimoto et al. [2003a], the author proposed inter-sample disturbance rejection (IDR) control to cancel high order RRO, where the periodic disturbance was modeled as Fourier series and the unknown amplitude and phase were estimated by the observer. This method was very effective when the number of selected modes is small to cancel the several disturbance modes. However, when the number is not small enough, the on-line computation cost of the observer is not negligible. In this section, a novel repetitive control is proposed based on perfect tracking controller (PTC) [Fujimoto et al., 2001] with periodic signal generator (PSG) [Kempf et al., 1993]. Because the PSG can be constructed by the series of memories z^{-1}, the computation cost is very low.

First, the PTC is designed using multirate feedforward control as minor-loop system to obtain the ideal command response. The measured output $y[i]$ is assumed to have the output disturbance $d[i]$ as

$$y[i] = p[i] - d[i] := \boldsymbol{c}\boldsymbol{x}[i] - d[i], \tag{7}$$

where $p[i]$ is the plant output [1]. In this section, the disturbance is assumed to be repetitive signal with

[1] In the application to HDD, $p(t)$ is the head position, $d(t)$ is the track runout, and $y(t)$ is the position error.

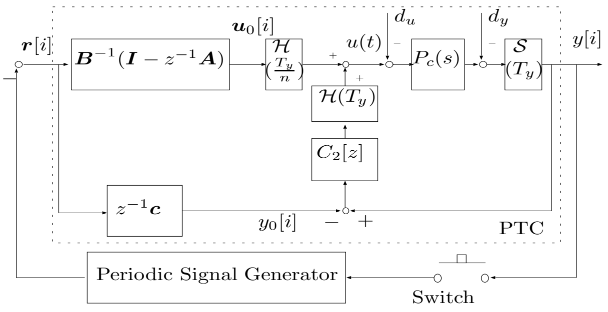

Fig. 2. Repetitive perfect tracking controller.

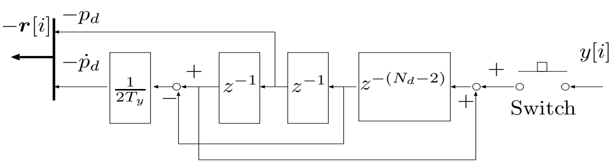

Fig. 3. Periodic signal generator for 2nd order system.

period T_d. From (4), the transfer function from $\boldsymbol{x}[i+1] \in \boldsymbol{R}^n$ to the multirate input $\boldsymbol{u}[i] \in \boldsymbol{R}^n$ can be derived as

$$\boldsymbol{u}[i] = \boldsymbol{B}^{-1}(\boldsymbol{I} - z^{-1}\boldsymbol{A})\boldsymbol{x}[i+1] \tag{8}$$

$$= \left[\begin{array}{c|c} \boldsymbol{O} & -\boldsymbol{A} \\ \hline \boldsymbol{B}^{-1} & \boldsymbol{B}^{-1} \end{array}\right] \boldsymbol{x}[i+1]. \tag{9}$$

From the definition in (6), the nonsingularity of matrix $\boldsymbol{B}$ is assured for a controllable plant. From (9), all poles of the transfer function (8) are zero. Hence, (8) is a stable inverse system. Then, if the control input is calculated by (10) as shown in Fig. 2, perfect tracking is guaranteed at sampling points for the nominal system because (10) is the exact inverse plant [Fujimoto et al., 2001].

$$\boldsymbol{u}_0[i] = \boldsymbol{B}^{-1}(\boldsymbol{I} - z^{-1}\boldsymbol{A})\boldsymbol{r}[i] \tag{10}$$

Here, $\boldsymbol{r}[i](:= \boldsymbol{x}_d[i+1])$ is previewed desired trajectory of plant state. The nominal output can be calculated as

$$y_0[i] = \boldsymbol{c}\boldsymbol{x}_d[i] = z^{-1}\boldsymbol{c}\boldsymbol{r}[i]. \tag{11}$$

When the tracking error $y[i] - y_0[i]$ is caused by unmodeled disturbance or modeling error, it can be attenuated by the robust feedback controller $C_2[z]$, as shown in Fig. 2.

Second, the periodic signal generator is designed to generate desired trajectory $\boldsymbol{r}[i]$. Because perfect tracking ($\boldsymbol{x}[i] = \boldsymbol{x}_d[i]$ or $\boldsymbol{x}[i] = z^{-1}\boldsymbol{r}[i]$) is assured, the minor-loop nominal system is expressed as

$$y[i] = z^{-1}r[i] - d_2[i], \; r[i] := \boldsymbol{c}\boldsymbol{r}[i], \tag{12}$$

where $d_2[i] := (1 - P[z]C_2[z])^{-1}d[i]$ and $P[z]$ is the single-rate plant with T_y if the minor-loop feedback controller $C_2[z]$ is a single-rate system. In the proposed RPTC, two schemes can be considered: the feedback and feedforward approaches. In case of feedback scheme (FB–RPTC), the switch of

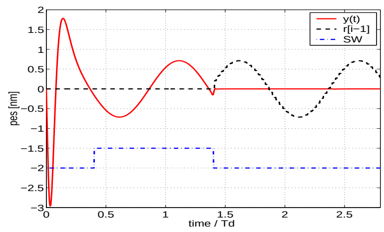

Fig. 4. FF–RPTC algorithm.

Fig. 2 is always on-state. The PSG can be designed as the outer-loop controller by

$$r[i] = -\frac{z}{z^{N_d} - 1}y[i], \tag{13}$$

where the integer N_d is defined as T_d/T_y. From (12) and (13), the total closed-loop system is represented by

$$y[i] = -\frac{z^{N_d} - 1}{z^{N_d}}d_2[i] \tag{14}$$

Therefore, the repetitive disturbance which is modeled as $d[i] = (z^{N_d} - 1)^{-1}$ is completely rejected at every sampling point in steady-state.

In (12), there exists redundancy to decide $\boldsymbol{r}[i] \in \boldsymbol{R}^n$ from the PSG output $r[i]$ since we have freedom to select the state variable $\boldsymbol{x}$. In order to make the multirate input smooth, it should be given as the derivative form $\boldsymbol{x} = [p, \dot{p}, \ddot{p}, \cdots]$. Fig. 3 shows one example of the 2nd order plant with $\boldsymbol{x} = [p, \dot{p}]$, in which the velocity command is generated by $\dot{p}_d[i] = (p_d[i+1] - p_d[i-1])/2T_y$.

However, the internal model (13) damages the closed-loop characteristics such as stability robustness since the gain of PSG becomes infinity at high order harmonics of periodic disturbance. Therefore, the feedforward algorithm of RPTC (FF–RPTC) is proposed with switching mechanism. Fig. 4 is a simple simulation result to explain this algorithm. The single mode disturbance of 70 [Hz] sinusoidal signal is added with 20 [nm] amplitude. The other simulation condition is almost same with the next section.

The disturbance is injected at $t = 0$ when the switch of Fig. 2 takes off-state. After the transient response of the minor-loop system with $C_2[z]$ and $P_c(s)$, the measured output $y[i]$ becomes steady-state response. Then, the switch turns on to store the output during one disturbance period T_d. After that, it turns off and keeps off-state. By using the stored signal, the PSG can reproduce the feedforward signal $\boldsymbol{r}[i]$ expressed in (13), as long as the disturbance is periodic. The dashed line of Fig. 4 means $y_0[i](= r[i-1])$. Here, the PTC generates control input $u_0[i]$ to cancel the periodic steady error. Thus, the plant output $p[i]$ perfectly tracks the periodic disturbance $d[i]$ and the tracking error becomes zero at every sampling point ($y[i] = 0$).

Since the switch turns on just N_d sampling time, the N_d memories work as complete feedforward

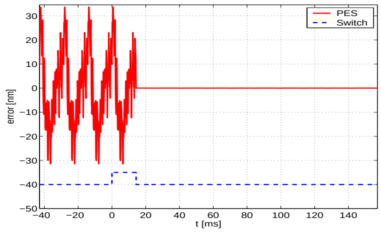

Fig. 5. FF (nominal plant: $k_p = 1.0k_{pn}, L = 0[\mu s]$)

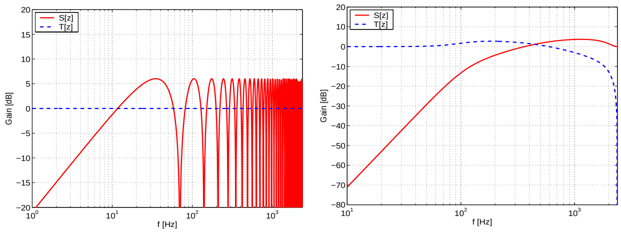

(a) FB–RPTC (b) FF–RPTC

Fig. 6. Sensitivity functions $S[z], T[z]$

compensator. Therefore, the disturbance can be rejected at every sampling point without sacrifice of the feedback characteristics. Note that the signal $y_0[i]$ is generated to prevent the additional transient response after the switch turns off.

3. APPLICATIONS TO RRO REJECTION IN HDD

3.1 Control system design and simulations

In the track-following mode of HDD, two kinds of disturbance which is injected at the plant output should be considered; repeatable runout (RRO) and non-repeatable runout (NRRO). While RRO is synchronous with the disk rotation, NRRO is not synchronous. Although there are many techniques to reject the RRO in low frequency region [Kempf et al., 1993], the high frequency RRO is hard to reject by conventional technologies. However, the effect of high-order RRO cannot be neglected since the required servo accuracy is getting drastically severe. Therefore, this paper applies the proposed multirate repetitive controllers both to FB and FF–RPTC.

The plant is a 2.5-in prototype HDD with 450[nm] track pitch. The sampling period of this drive is $T_y = 210.08$ [μs], and the control input is changed $N = 2$ times during this period. In the design of controller, the nominal plant $P_n(s)$ is modeled as double integrator system. The simulation model $P_a(s)$ includes the dead-time and gain variation as follows.

$$P_n(s) = \frac{k_{pn}}{ms^2}, \quad P_a(s) = \frac{k_p}{ms^2}e^{-Ls} \tag{15}$$

The rotation frequency of spindle motor is 70[Hz] and the number of sector is $N_d = 68$. The minor-loop FB controller $C_2[z]$ is designed by the lead-lag compensator with 450[Hz] cross-over frequency.

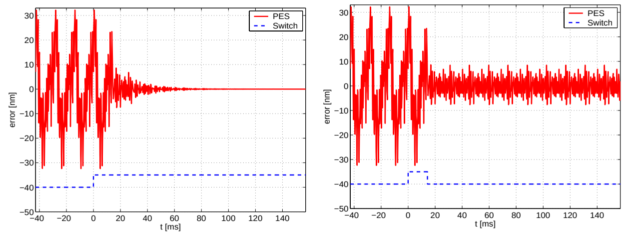

(a) FB–RPTC (b) FF–RPTC

Fig. 7. Small variation
($k_p = 1.1k_{pn}, L = 43.26[\mu s]$)

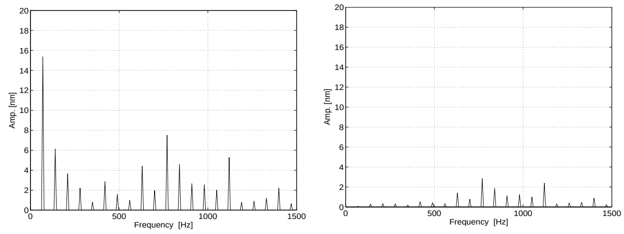

(a) Before compensation (b) After compensation

Fig. 8. FFT of Fig. 7(b)

Fig. 5 $\sim$ 9 shows the simulation results. The injected disturbance signal is calculated from the approximate inverse of sensitivity function and position error signal (PES) obtained from experiments. As the effect of NRRO is considered in the next experiments, the simulations use the only RRO signal which is extracted from experimental data by the averaging operation of total PES.

Fig. 5 shows the time response of FF–RPTC for the nominal plant. The time origin ($t = 0$) is at the instance that the switch turns on to start the compensation. While the swith takes on-state only one disturbance period $T_d = 14.3$[ms] in FF–RPTC, the FB–RPTC keeps the on-state all the time. As shown in Fig. 5, the PTC works from $t = T_d$ to perfectly tracks the RRO with zero error.

Fig. 6 shows the sensitivity $S[z]$ and complementary sensitivity $T[z]$ of the total closed-loop systems including PSG. In FB–RPTC, the sensitivity is zero at the harmonics of 70 [Hz] as (14) since the PSG is the internal model of the periodic disturbance. On the other hand, since the PSG becomes pure feedforward controller in FF–RPTC as stated above, the closed-loop characteristics are determined by the minor-loop with $C_2[z]$ and $P[z]$. Thus, the fine closed-loop frequency response can be reserved by the $C_2[z]$ which can be designed independently.

Fig. 7 is the case with the dead-time $L = 43.26[\mu s]$ and small gain variation of 10[%]. Although the little oscillation is generated, the error of FB–RPTC converges to zero by internal model principle. However, the tracking performance is worsen by the plant variation in FF–RPTC. To investigate the reason, the FFT analysis of Fig. 7(b) is shown in Fig. 8. The figure (b) is obtained form the PES after the switch turn on and the

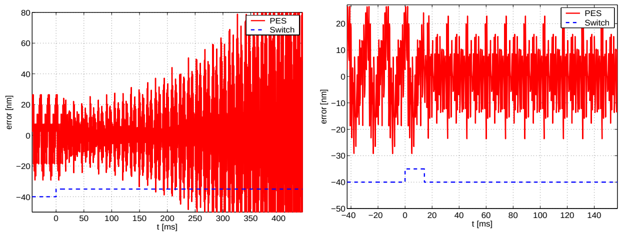

(a) FB–RPTC (b) FF–RPTC

Fig. 9. Big variation ($k_p = 1.4k_{pn}, L = 43.26[\mu s]$)

figure (a) is without the compensation. In the feedforward control, the variation of command response against plant variation is determined by the sensitivity $(1-P[z]C_2[z])^{-1}$ which is shown in the solid line of Fig. 6(b). Thus, the performance becomes poor in high sensitivity band while the RRO is attenuated well in control bandwidth. In order to overcome this drawback of feedforward control, the author has proposed the adaptive technique [Fujimoto et al., 2003b] to reduce the modeling error and to recover the performance.

Fig. 9 shows the simulation results with big gain variation of 40[%]. FB–RPTC becomes unstable since the stability robustness is worsen by PSG which has infinite gain at harmonic frequencies. This can also be understood from the complementary sensitivity shown in Fig. 6(a) that has no roll-off in high frequency. On the other hand, the FF–RPTC can keep the stability for the big plant uncertainty, as shown in Fig. 9(b).

3.2 Experiments on RPTC

In this section, the proposed methods are verified through experiments. The experiments of FB–RPTC became unstable since it had small stability margin as stated above. To make it stable, we need a low-pass filter (LPF) to eliminate the peak gain at high-order modes and to assure the stability robustness. Thus, the specific LPF called Q–filter [Chew and Tomizuka, 1990] is implemented as

$$p_f[i] = \frac{z+\gamma+z^{-1}}{\gamma+2}p_d[i] \qquad (16)$$

$$\dot{p}_f[i] = \frac{z+\gamma+z^{-1}}{\gamma+2}\dot{p}_d[i], \qquad (17)$$

where $\boldsymbol{r}[i] = [p_f[i], \dot{p}_f[i]]^T$ is utilized instead of $= [p_d[i], \dot{p}_d[i]]^T$ in Fig. 2. The smaller $\gamma(\geq 2)$ has bigger roll-off and bigger stability although the disturbance rejection performance becomes poorer [Chew and Tomizuka, 1990]. The frequency response of Q–filter is shown in Fig. 10. On the other hand, this LPF is not required in the proposed FF–RPTC because of the switching scheme.

Experimental results both of FB and FF–RPTC are shown in Fig. 11 $\sim$ 13. In FF–RPTC, the RRO signals which are averaged with respect to the sector number are stored in the PSG. The figures (a) are only with the lead-lag compensator as $C_2[z]$. The figures (b) and (c) are the FB and FF–RPTCs, respectively. From Fig. 11(b), we find that the RRO components of FB–RPTC are almost zero because of the internal model principle. On the other hand, the proposed FF–RPTC has small position error which is caused by the modeling error of the plant. This is the disadvantage of feedforward approach.

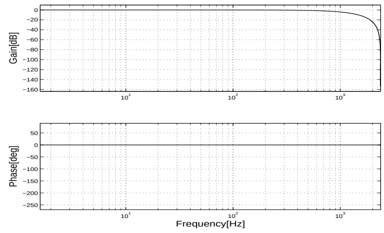

Fig. 10. Q–filter. ($\gamma = 2$)

As shown in Fig. 12(b), however, NRRO components of FB–RPTC are greatly amplified than the original $C_2[z]$ of Fig. 12(a). The reason is that the internal model worsens the total sensitivity function in NRRO frequencies by the Bode's integral theorem, as shown in Fig. 6(a). Since the FF–RPTC overcomes this problem by the switching mechanism, Fig. 12(c) has the almost same response with Fig. 12(a). As shown in Fig. 13, the total tracking accuracy is improved 32.6 % by the proposed switching methods as $\pm3\sigma$=51.5[nm], although that of the FB–RPTC is worsen 19.8 % than the original $C_2[z]$.

4. CONCLUSION

In this paper, two switching based repetitive controllers named FB–RPTC and FF–RPTC were proposed to reject high-order repetitive disturbances. The advantages and disadvantages of these schemes were discussed. By internal model principle, the FB approach can assure the convergence to zero tracking error against the small plant variation as long as the stability robustness is reserved. However, it needs Q–filter to keep the stability in the experiments. Moreover, it amplifies the NRRO since the total sensitivity is worsen by the internal model. These disadvantages are not only for the FB–RPTC but also for all the conventional repetitive controllers which have one-degree-of-freedom structure.

On the other hand, the FF–RPTC enabled the feedforward controller to make the repetitive compensation by the switching mechanism. Thus, the stability robustness can be preserved by the independent feedback controller. However, the performance robustness of periodic disturbance rejection is worsen over the minor-loop bandwidth.

The future works will be the reduction of modelling error by the adaptive scheme and dead-time compensation, and effective rejection of NRRO.

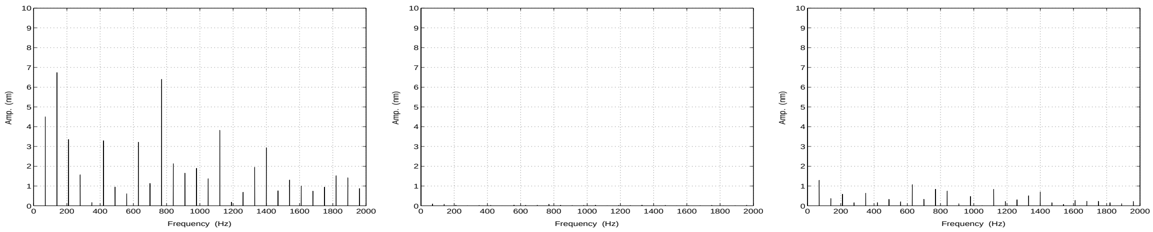

(a) Lead-Lag only (b) FB–RPTC (c) FF–RPTC

Fig. 11. Experimental results of RPTC. (RRO components)

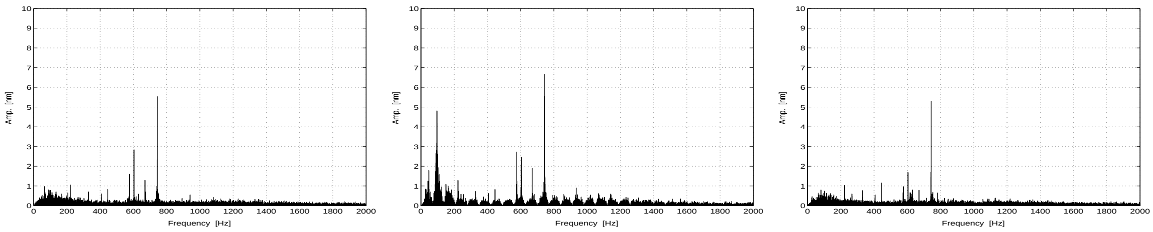

(a) Lead-Lag only (b) FB–RPTC (c) FF–RPTC

Fig. 12. Experimental results of RPTC. (NRRO components)

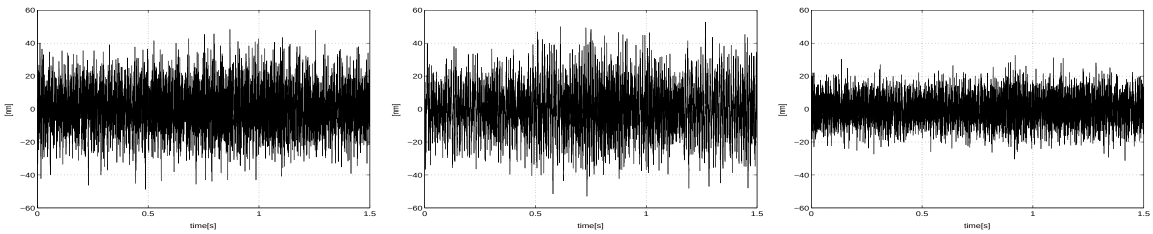

(a) Lead-Lag ($\pm 3\sigma$=76.4[nm]) (b) FB–RPTC($\pm 3\sigma$=91.5[nm]) (c) FF–RPTC($\pm 3\sigma$=51.5[nm])

Fig. 13. Experimental results of RPTC. (time response)

Finally, the authors wish to thank Dr. S. Nakagawa and Dr. A. Okuyama of Hitachi for their support and the author's former student, Mr. F. Kawakami, for the helps in experiments.

REFERENCES

Chew, K.K. and M. Tomizuka (1990). Digital control of repetitive errors in disk drive systems. *IEEE Contr. Syst. Mag.*, 10(1):16–20.

Fujimoto, H., Y. Hori and A. Kawamura (2001). Perfect tracking control based on multirate feedforward control with generalized sampling periods. *IEEE Trans. Industrial Electronics*, 48(3):636–644.

Fujimoto, H., Y. Hori, T. Yamaguchi and S. Nakagawa (1999). Proposal of perfect tracking and perfect disturbance rejection control by multirate sampling and applications to hard disk drive control. In *Conf. Decision Contr.*, pages 5277–5282.

Fujimoto, H., F. Kawakami and S. Kondo (2003a). Multirate repetitive control and applications – verification of switching scheme by HDD and visual servoing –. In *Amer. Control Conf.*, pages 2875–2880.

Fujimoto, H., F. Kawakami and S. Kondo (2003b). Repetitive control of hard disk drive based on switching scheme and gain adaptation. In *IEE of Japan Technical Meeting Record*, number IIC-03-92, pages 1–6.

Hara, S., Y. Yamamoto, T. Omata and M. Nakano (1988). Repetitive control system – a new-type servo system. *IEEE Trans. Automat. Contr.*, 33:659–668.

Hirata, M., M. Takiguchi and K. Nonami (2003). Track-following control of hard disk drives using multi-rate sampled-data H_∞ control. In *Conf. Decision Contr.*, pages 3414–3419.

Kempf, C., W. Messner, M. Tomizuka and R. Horowitz (1993). Comparison of four discrete-time repetitive algorithms. *IEEE Contr. Syst. Mag.*, 13(5):48–54.

Lee, D.J. and M. Tomizuka (2003). Multirate optimal state estimation with sensor fusion. In *Amer. Control Conf.*, pages 2887–2892.

Takakura, S. (1999). Design of the tracking system using N-Delay two-degree-of-freedom control and its application to hard disk drives. In *IEEE Conf. Control Applications*, pages 170–175.

Tomizuka, M. (1987). Zero phase error tracking algorithm for digital control. *ASME, J. Dynam. Syst., Measur., and Contr.*, 109:65–68.

Wu, S.C. and M. Tomizuka (2003). Multi-rate digital control with interlacing and its application to hard disk drive servo. In *Amer. Control Conf.*, pages 4347–4352.